On the Structure Sensitivity of CO Oxidation on Alumina Supported Pd–Pt Bimetallic Catalysts

Sarp KAYA[1,2]**, Ebru ERUNAL**[1,3]**, Riad SHALTAF**[4,5]**,**
Şinasi ELLİALTIOĞLU[4] **and Deniz UNER**[1,*]

[1]*Department of Chemical Engineering, Middle East Technical University,*
Ankara, 06531 TURKEY
e-mail: uner@metu.edu.tr
[2]*Present Address: Stanford Linear Accelerator Center, 2575 Sand Hill Road, Menlo Park,*
CA 94025, USA
[3]*Present Address: Albert-Ludwigs Universität, Inst. für Phys.Chem.1, Albertstr. 21, 79104,*
Freiburg im Breisgau, GERMANY
[4]*Department of Physics, Middle East Technical University, Ankara, 06531 TURKEY*
[5]*Present Address: Unité Physico-Chimie et de Physique des Mat'eriaux (PCPM)*
Université catholique de Louvain UCL/SE/FSA/MAPR/PCPM
Louvain-la-Neuve, BELGIUM

CO oxidation reaction was studied over monometallic and bimetallic palladium–platinum catalysts at 25:75, 50:50, and 75:25 Pd:Pt atomic fractions co-impregnated over a γ-Al_2O_3 support. The size of the metal particles, measured by modified hydrogen chemisorption, increased as the Pd fractions in the catalyst increased. The surface compositions and site metal distributions of the catalysts determined from Monte Carlo simulations indicated that Pd atoms segregated to the surface: at low Pd levels, Pd occupied preferentially 6 and 7 coordinated defect-like sites. As the Pd fraction increased, first 8 coordinated (100) and then 9 coordinated (111) planes were populated. At low temperatures (below 423 K), CO oxidation reaction over bi-metallic catalysts behaved like the monometallic Pd catalyst suggesting that Pd atoms segregated to the surface. The results of Monte Carlo studies and reaction tests together were interpreted as the governing steps in CO oxidation primarily taking place at the defect-like sites.

Key Words: CO oxidation, bimetallic catalysts, palladium, platinum, surface segregation, Monte Carlo simulation.

*Corresponding author

Emission control technologies from mobile sources heavily rely on precious metals, especially Pt. To overcome price fluctuations in the precious metal market, Pd was used as an alternative to Pt in oxidation catalysts. Presently, Pd-Pt bimetallic catalysts are frequently employed in the oxidation catalyst formulations. In addition to lower costs, the synergy between Pt and Pd in bimetallic catalysts offers an additional advantage. It was already reported in the literature that the bimetallic catalysts showed better performance than the monometallics in methane combustion reaction[1,2,3,4,5]. Strobel et al.[2] suggested that the addition of small amounts of platinum made the palladium particles more resistant against sintering at high temperatures and further lowered the deactivation observed during methane combustion. Persson et al.[3] proposed that adding small amounts of platinum into the palladium catalyst improved activity in comparison to the monometallic palladium catalyst but also higher amounts of platinum were required for stabilizing the methane conversion. They reported that the most promising catalysts with respect to both activity and stability were $Pd_{67}Pt_{33}$ and $Pd_{50}Pt_{50}$. Liotta et al.[4] observed an enhancement in the catalytic activity towards methane combustion with the Pd-Pt (atomic ratio - 1:1) addition to their special type honeycomb supported Co_3O_4/CeO_2 catalysts for CO/CH_4 emission abatement. They also mentioned that this type of catalyst exhibited excellent cold start activity with massive CO conversions below 100 $^\circ$C under lean burn conditions. Lapisardi et al.[5] reported that partial substitution of Pd with Pt on Al_2O_3-supported Pd catalysts led to improved performance in catalytic oxidation of methane under lean-burn conditions, especially in the presence of large amounts of water vapor. Pd-Pt/CeO_2 catalysts were also tested for their activities in the selective CO oxidation reactions, demonstrating that 1:7 Pt:Pd mixture exhibited the best activity and highest dispersions.[6]

The preparation method is a significant factor influencing the formation of intimate mixtures as well as alloys. For example, after sequential impregnation over γ-Al_2O_3 with intermediate calcination, monometallic clusters are synthesized.[7] On the other hand, over beta zeolite supports, it was shown that the order of impregnation could determine the formation of alloys: impregnating Pd first and then impregnating Pt could produce more alloys compared to when impregnation order was reversed or when co-impregnation was used.[8,9]

In this study, our aim is to understand the catalytic activities of Pd-Pt bimetallics towards CO oxidation reaction. Once bimetallic particles are formed, modified catalytic activities are expected owing to the factors involving atomic fractions at the topmost surface, particle size, and dispersions. Even though Pd-Pt bimetallics were shown as active systems for some combustion and hydrogenation reactions, their catalytic activities towards CO oxidation reaction has not been studied in terms of the relationship between the active sites and the surface compositions. In order to do this, the CO oxidation activities of supported Pt-Pd bimetallic catalysts were monitored while their surface compositions determined from Monte Carlo simulations were used to interpret CO oxidation light-off data.

Methods

Catalyst preparation

The incipient wetness technique was used to prepare alumina impregnated monometallic and bimetallic palladium and platinum catalysts. 1 wt % of Pd, Pt, or Pd–Pt were loaded onto the gamma-alumina (γ-Al_2O_3) supports by impregnating the supports with sufficient precious metal precursor solution to bring about incipient wetness ($\sim$1–2 ml solution/g support). For bimetallic catalysts, Pd–Pt atomic fractions were selected as 25:75,

50:50, and 75:25. The catalysts were prepared via co-impregnation of Pd and Pt from $Pt(NH_3)_4Cl_2.H_2O$ (Johnson Matthey) and $PdCl_2$ (Johnson Matthey). The catalysts were then dried at room temperature for 6 h and at 393 K for 12 h. Finally, they were calcined at 723 K for 4 h. A part of these catalysts was used as such, and the other part was washed with hot distilled water ($\sim$350 K) until it was free of Cl^- ions tested by $AgNO_3$ solution then again calcined at 673 K for 4 h.[10]

Catalysts characterization

The active metal dispersions were determined by measuring strong hydrogen amounts at 298 K measured via a modified volumetric chemisorption technique.[11] The adsorption experiments were performed in a manifold described elsewhere.[12] Prior to reduction, about 2 g of catalyst was heated up to a temperature of 423 K and kept at that temperature for 30 min under vacuum (10^{-4} Torr). The samples were reduced under static hydrogen at 623 K for a total duration of 2 h, evacuating and replenishing hydrogen every 20–25 min. At the end of the reduction period, the manifold was evacuated and the sample was cooled, then total and weak hydrogen isotherms were measured. The dispersions were calculated assuming a strong hydrogen stoichiometry of H / Pd = 1 or H / Pt = 1.

Monte Carlo Simulations

The canonical Monte Carlo simulation was used where the number of particles (N), volume (V), and temperature (T) were fixed following the work of King.[13,14,15,16] Although the King's group has published a more rigorous thermodynamic approach for the determination of surface segregation phenomena in multimetallic catalytic single crystal materials,[17] the Monte Carlo method allowed us predict compositions of the clusters as a function of bulk and surface coordination. Since the method is finely described in the original publications, and also thoroughly reviewed,[16] it will be covered here only briefly.

The model requires the determination of constants a^i, b^i, and c^i for a semi-empirical partial bond energy function, which is a function of the coordination, n, of the ith atom:

$$\varepsilon_n^i = a^i + b^i n + c^i n^2 \tag{1}$$

The energy associated with the pair-wise interaction between the species i with coordination n and its nearest neighbor j with coordination m will be $\varepsilon_n^i + \varepsilon_m^j$. For the accurate treatment of the alloys, the interchange energy ω_{ij} and the coordination number Z for the bulk should also be accounted for:

$$E_{ij} = \frac{\omega_{ij}}{Z} + (\varepsilon_n^i + \varepsilon_m^j) \tag{2}$$

The interchange energy was determined from the ΔG_{mix}^{ex} data of Myles and Miller for bulk Pd-Pt alloys.[18] The interchange energy was taken as invariant with composition, coordination, and temperature. The constants a^i, b^i, c^i are determined from the empirical data of heat of sublimation,[19] vacancy formation energy,[20] and the surface energy of (100) plane.[20] The thermodynamic data collected from the literature[21,22] are presented in Table 1. The semi-empirical constants determined from these data are presented in Table 2. Initially, the atoms were distributed randomly in the cluster of a given size, which was assumed to be in cubo-octohedral

shape as its equilibrium geometry. Then the Monte Carlo procedure was applied by randomly picking each time 2 neighboring atoms of different types and calculating the difference in the final energy, ΔE, of the system due to the exchange of their positions. The new configuration was accepted or rejected according to the sign of ΔE following the standard Metropolis algorithm.[23] The procedure was repeated until the system reached equilibrium, i.e., no significant changes in total energy due to any exchange of neighbors, was no longer observed, i.e., when the system was considered to have reached equilibrium.

Table 1. Thermodynamic properties of palladium and platinum.

Property	Palladium	Platinum
Melting point (K) [21]	1827.9	2041.4
Boiling point (K) [21]	3236	4098
Enthalpy of fusion (eV/atom) [21]	0.1734	0.2353
ΔH_{sub} (eV/atom)	3.9074 [19]	5.8565 [16]
E_v (eV/atom)	1.26 [20]	1.35 [16]
$\sigma_{(100)}$ (eV/atom)	1.2002 [20]	3.8363 [16]
a_0(Å)	3.886 [22]	0.797 [16]

Table 2. The constants of Eq. (1) derived from thermodynamic parameters to be used in Monte Carlo simulations.

Parameter	Palladium (Calculated)	Platinum [16]
a^i	–0.17	–0.4015
b^i	–0.049	–0.05232
c^i	0.003	0.003759
ω_{ijz}/Z(eV)	–0.004	

Activity measurements

CO oxidation activities over the catalysts were conducted in a horizontal fixed-bed reactor made of a quartz tube (13 mm ID) under atmospheric pressure. One hundred milligram catalyst diluted with 900 mg γ-Al$_2$O$_3$ was placed in the reactor. The catalyst bed was supported by quartz wool at both ends. A thermocouple was placed externally with one end touching the catalyst zone in order to measure the bed temperature. The quartz reactor was placed inside a temperature controlled tubular oven. The temperature of the oven was increased from room temperature to the reaction temperature (approximately 350 K) then the catalysts were conditioned with a stoichiometric gas mixture 5% CO, 2.5% O$_2$, and N$_2$ for 30 min. Inlet gas compositions were controlled by MKS 1179A mass flow controllers and the analysis of the product gases was carried out using an on-line gas chromatograph (HP 4890) equipped with a thermal conductivity detector (TCD) and a Porapak Q column. The total gas flow rate through the reactor was kept constant at 200 ml/min. Effect of bimetallic interaction on CO oxidation reaction was studied by dynamic light-off experiments. The catalyst bed was heated at a rate of 1 K/min and CO consumption and CO$_2$ formation rates were monitored with the gas chromatograph until 100%

CO conversion was obtained. The reaction orders with respect to carbon monoxide and oxygen were measured at the temperatures where CO conversion was below 5% so that differential reactor assumption was valid.

Results and Discussion

Characterization of monometallic and bimetallic Pd and Pt catalysts

Active site characterizations of all catalysts were performed by the volumetric hydrogen chemisorption technique at ambient temperature. It is well known that palladium and hydrogen can form β-hydride species, so the dispersion measurements are based on the data collected below 10 Torr hydrogen pressure in order to minimize discrepancies due to hydride formation. In this pressure range the spillover effect is also minimized. Below 10 Torr, it was assumed that hydrogen molecules were only chemisorbed to the metals. Active metal dispersions of monometallic and bimetallic catalysts were calculated assuming 1:1 stoichiometry of H:M (M: Pd or Pt). For bimetallic catalysts, calculated dispersions were based on weighed averages of the atomic masses of palladium and platinum metals. The dispersions of all monometallic and bimetallic catalysts are given in Table 3. Hydrogen adsorption isotherms of washed catalyst samples showed that Pd:Pt (75:25) catalyst had the lowest hydrogen adsorption capacity. The decrease of metal dispersions upon washing was especially significant for bimetallic catalysts. This decrease was attributed to sintering of particles during the second calcination after washing. One point to mention here is that for these catalysts, the amount of surface metal atoms/g catalyst was almost the same for all of the catalyst compositions despite the significantly different dispersions for Pd and Pt containing catalysts.

Monte Carlo simulations

The Monte Carlo simulations were conducted for different compositions of Pt and Pd and for different cluster sizes. The cluster size was set by the shape of the cubo-octahedral structures as containing 201, 586, 1289, and 2406 atoms. The estimations of the simulations were compared with the published experimental data[24] for the smallest and largest clusters investigated in this work. The simulations slightly overestimate the surface compositions in comparison to the experimental data especially at low temperatures. At 600 K, more than 80% surface Pd enrichment was observed experimentally; however, simulations converged to Pd surface fractions close to 90% at all cluster sizes studied. Better agreement was obtained at higher temperatures suggesting that kinetic limitations might play a role in equilibrium surface Pd fractions. At 1000 K, ~95% Pd surface fraction found experimentally was also confirmed with simulations. It should be noted that at low temperatures, it takes much longer to achieve the true equilibrium, especially in the solid phases, thus slight deviations between the reported experimental data and simulations are not entirely unexpected at low temperatures. The effect of the cluster size on the average surface composition is presented in Figure 1. There is a slight but non-negligible enrichment of the surface with Pd as the dispersion of the catalyst increased, especially at higher Pd loadings. Furthermore, the data in Figure 1 clearly demonstrates that the surface is enriched by Pd in comparison to the bulk compositions shown in the legend of the figure. The segregation behavior of Pd has been anticipated and also has been demonstrated experimentally[25] and theoretically.[25,26] The surface compositions as a function of the coordination number of the sites are presented in Figure 2. It is clearly seen that Pd preferred to populate

the edge (6 coordinated) and corner (7 coordinated) sites at low loadings. It is important to note that even at Pd loadings of 25%, more than 80% of 6 and 7 coordinated atoms were populated by Pd.
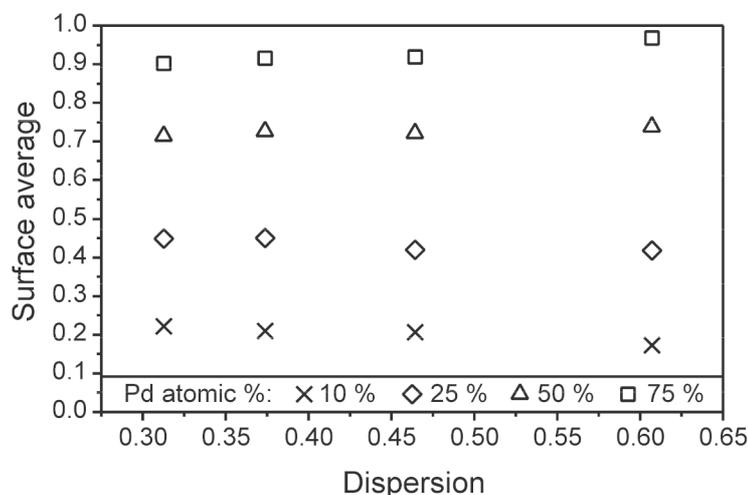

Figure 1. The effect of the particle dispersion on predicted surface fraction of Pd at 800 K.
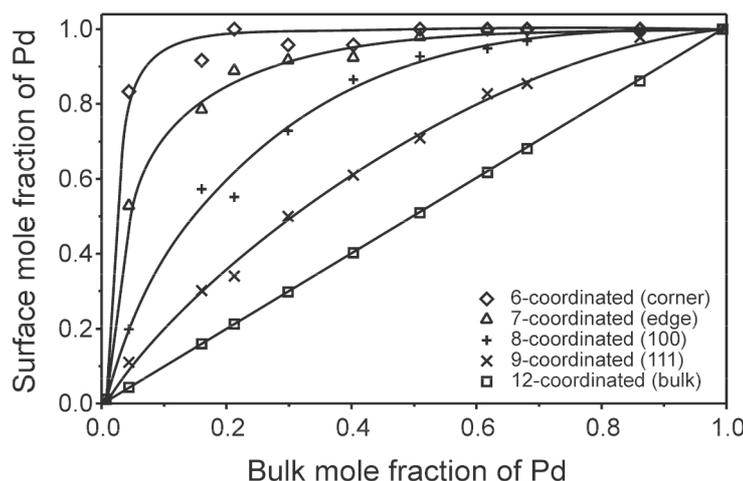
Figure 2. Pd atom population distribution between the different surface terminations of a 2406-atom cluster as a function of bulk composition (T=800 K).

In order to be able to visualize the relative distributions of Pd and Pt, the simulated particles with dispersions closest to the experimentally determined values are shown in Figure 3. It is important to note here that the particle size in Monte Carlo simulations can be incremented by adding one full shell of atoms, thus the dispersion increments are dictated by these particle sizes. On the other hand, for the real catalysts, experimentally measured dispersion values represent an average value of a distribution of the metal particle sizes. Thus, the closest possible particle sizes to the experimentally determined dispersions were selected from the results of the Monte Carlo simulations. The particles presented in Figure 3 indicate the population of defect-like edge and corner sites by Pd at all compositions and all dispersions. The data presented in Figure 3

16

and Table 3 were also compiled in Table 4 for reference. The results presented so far is quite consistent with the surface concentration profiles measured for the 3 low-index surfaces of Pd–Pt (1:1) random alloys at 500, 1000, and 1500 K by EXAFS technique.[25] Similar to our findings, Monte Carlo simulations for the structure of a 55-atom cluster of Pd-Pt bimetallic catalyst revealed that Pd segregated on the surface in the following order: as Pd concentration increased, the vertices, then the edge of outer shell, then the center of the cluster, and finally the interior shell occupied by Pd.[26]
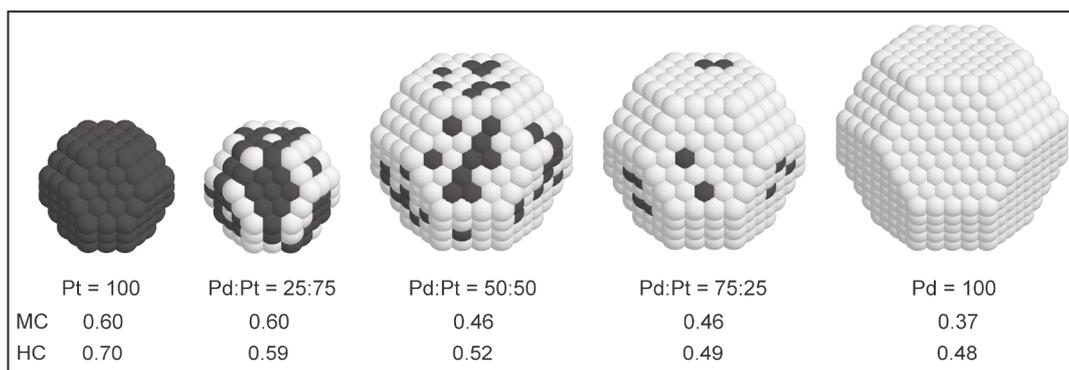
Figure 3. Monte Carlo predicted Pt-Pd clusters at the compositions used in the experimental work. The cluster sizes were based on the hydrogen chemisorption data. Dark and light atoms represent Pt and Pd, respectively. (MC: Dispersions based on Monte Carlo simulations, HC: Dispersions measured by hydrogen chemisorption).

Table 3. Dispersion values of palladium and platinum monometallic and bimetallic catalysts based on strong hydrogen chemisorption.

Pd:Pt	Unwashed Dispersion, %	Washed Dispersion, %	Unwashed, μmole of surf. cat.	Washed, μmole of surf. cat.
0:100	70.4	60.8	36.1	31.2
25:75	57.8	39.6	33.4	22.9
50:50	52.3	38.3	34.7	25.4
75:25	49.1	23.5	38.2	18.3
100:0	47.9	27.9	45.0	26.2

Non-isothermal CO oxidation performances on alumina supported monometallic and bimetallic palladium-platinum catalysts

CO oxidation reaction on both monometallic and bimetallic catalysts was carried out under a stoichiometric gas environment by increasing the reactor temperature in the search of any synergy between Pd and Pt in this reaction system. In addition, the effects of residual chloride were investigated by testing the catalysts before and after washing.

Table 4. Comparison of the experimental dispersions of Pd-Pt bimetallic catalysts with the values estimated by MC simulations.

At.% Pd	Fractional dispersion of un-washed catalysts by volumetric chemisorption technique	Cluster size chosen based on the dispersion (number of atoms)	Fractional dispersion on the cluster	% of the surface sites occupied by Pd from simulations
0	0.70	201	0.60	0.00
25	0.58	201	0.60	0.42
50	0.52	586	0.46	0.72
75	0.49	586	0.46	0.91
100	0.48	1289	0.37	1.00

Unwashed catalysts

CO oxidation performances of unwashed, co-impregnated bimetallic catalysts followed a trend quite similar to the catalytic performance of monometallic palladium (Figure 4) due to the segregation of palladium to the surface. The light-off trends, up to 30% conversion, were identical for all bimetallic Pd–Pt catalysts and monometallic palladium followed the identical light-off trend in nearly the same temperature interval.
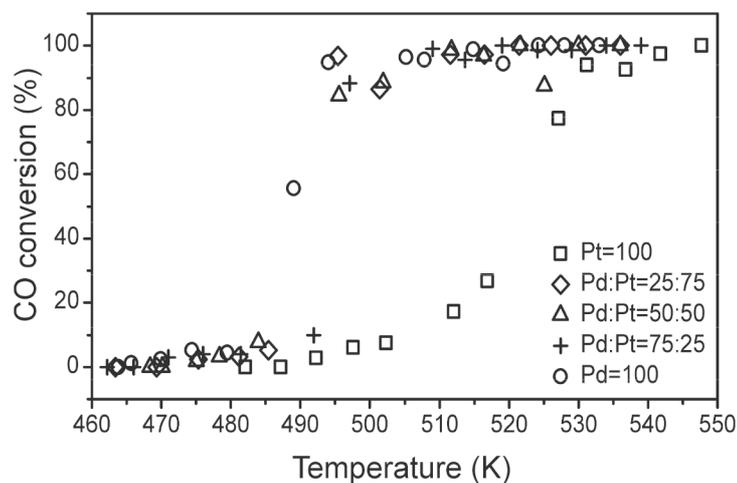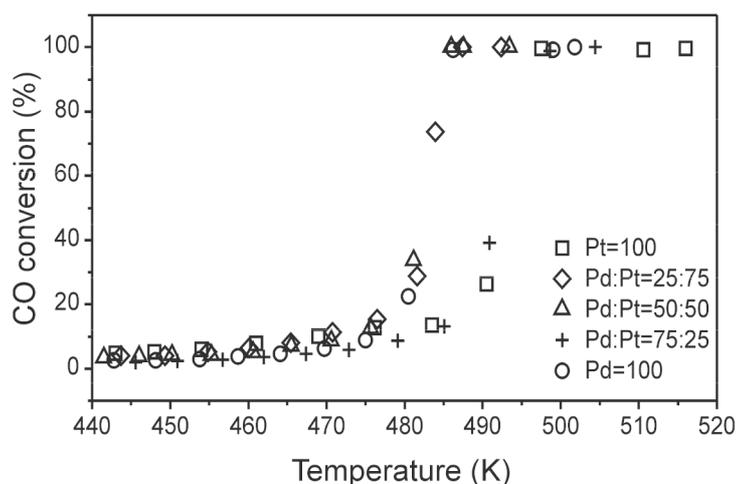

Figure 4. Light-off performances of the unwashed co-impregnated Pd-Pt catalysts. Feed gas composition: 5% CO, 2.5% O_2, balance N_2. $\dot{V}_{\text{total}} = 200$ ml/min.

Washed catalysts

CO oxidation performances of the catalysts after washing under stoichiometric feed gas compositions are shown in Figure 5. After washing, the performance gap between monometallic catalysts became narrower but the

performances of bimetallic Pd–Pt catalyst were still similar to monometallic palladium except for the 75% Pd:Pt bimetallic catalyst. All co-impregnated catalysts showed almost identical light-off performances up to 20% conversion. Furthermore, both reaction onset temperature and T_{50} values improved after washing. Since both palladium and platinum catalysts were prepared from chlorine containing metal salts, removal of residual chlorine apparently improved the performance of the catalysts. It is also important to note here that the dispersions of the catalysts decreased upon washing indicating particle sintering as a result of second calcination. The dispersion of 75% Pd containing co-impregnated catalysts decreased significantly upon washing and calcination (Table 3). The decrease of dispersion can explain the loss of activity of that particular catalyst in comparison to the other bimetallic catalysts (Figure 5).

Figure 5. Light-off performances of washed co-impregnated Pd-Pt catalysts. Feed gas composition: stoichiometric, 5% CO, 2.5% O_2, balance N_2. $\dot{V}_{total} = 200$ ml/min.

Apparent activation energies and orders

The reaction orders with respect to oxygen and CO partial pressures as well as the activation energies measured on our catalysts are presented in Table 5. There was no definitive trend in either orders or activation energies with respect to Pd amounts. The oxygen orders of bimetallic catalysts remained in between the orders measured for the monometallic catalysts while CO orders did not exhibit any indication of a change in reaction mechanism. The fluctuations in the activation energy data could be attributed to the slight changes in the temperature ranges at which these measurements were performed.

On the structure sensitivity

The results presented so far indicate that the Pd atoms in the bimetallic catalysts segregate to the surface with a strong preference towards the defect-like sites. The CO oxidation tests indicated that all the bimetallic catalysts behaved like monometallic palladium further confirming the segregation behavior of this metal. In fact, similar behavior was observed previously for methane, propane, and propene oxidation reactions.[9] Previous work in the literature and from our group[27,28,29] has clearly demonstrated the structure sensitivity of CO oxidation and

selective CO oxidation in PROX reactions. Under the conditions used in this work, apparently the structure sensitivity of CO oxidation is still prevalent. This is especially apparent at low Pd loadings where only defect-like sites seems to be populated by Pd (Figure 3). These results are consistent with the recent publications from Nørskov group indicating the role of the step sites in the activation of O_2 and CO.[30] We have previously demonstrated the structure sensitivity of dissociative oxygen adsorption over Pt/Al_2O_3 systems[31] where we changed the relative population of the defect-like sites by annealing. In the presence of higher number of defect sites, the integral adsorption heats and surface coverages of oxygen were indeed higher. The experimental results for co-impregnated Pd-Pt bimetallic catalysts indicated that all of the bimetallic catalysts behaved like monometallic Pd, in other words, the catalytic activity of Pd dominated over the surface. One further point to note here is regarding the role of the defects in the dissociation of oxygen molecule. On stepped Pt surfaces, it has been clearly demonstrated that the step sites played an important role in the oxygen dissociation, and therefore, in the overall reaction kinetics and measured activation energies of CO oxidation reaction.[32] In our previous work, we have demonstrated that the monometallic Pd was less sensitive to CO to oxygen stoichiometry than Pt.[7] When combined with the results of the Monte Carlo simulations, we conclude that the essential activity of CO oxidation under the conditions studied here is taking place at the defect-like sites.

Table 5. Reaction orders and activation energies of CO oxidation reaction. The activation energies were measured under a stoichiometric feed gas composition: 5% CO, 2.5% O_2, balance N_2. $\dot{V}_{total} = 200$ ml/min.

Pd:Pt	E_a measurement temperature range (K)	E_a (kJ/mole)	Reaction order measurement temperatures (K)	CO orders	O_2 orders
0:100	420–465	57.0	448	–0.8	1.8
25:75	425–465	47.1	440	–1.3	1.2
50:50	445–470	51.2	445	–0.6	1.3
75:25	425–480	67.9	450	–0.9	1.3
100:0	425–480	58.7	445	–0.9	0.8

Conclusions

CO oxidation reaction was studied over mono- and bi-metallic Pd–Pt catalysts. The bimetallic catalysts were prepared by co-impregnation. Monte Carlo simulations of bimetallic catalysts indicated that Pd segregated to the surface of the particles at all sizes and compositions. The segregation phenomenon was apparent during the CO oxidation reaction for bimetallic catalysts. Measured reaction orders and activation energies did not indicate any significant synergy. Furthermore, as the Pd loading increased, a decrease in dispersion was observed.

Acknowledgements

References

1. Persson, K.; Jansson, K.; Järås, S. G. *J. Catal.* **2007,** *245,* 401–414.

2. Strobel, R.; Grunwaldt, J.-D.; Camenzind, A.; Pratsinis, S. E.; Baiker, A. *Catal. Lett.* **2005,** *104,* 9–16.

3. Persson, K.; Ersson, A.; Jansson, K.; Fierro, J.L.G.; Järås, S.G. *J. Catal.* **2006**, *243,* 14–24.

4. Liotta, L.F.; Di Carlo, G.; Pantaleo, G.; Deganello, G.; Borla, E. M.; Pidria, M. *Catal. Commun.* **2007**, *8*, 299–304.

5. Lapisardi, G.; Urfels, L.; Gélin, P.; Primet, M.; Kaddouri, A.; Garbowski, E.; Toppi, S.; Tena, E. *Catal. Today* **2006**, *117*, 564–568.

6. Parinyaswan, A.; Pongstabodee, S.; Luengnaruemitchai, A. *Int. J. Hydrogen Energ.* **2006**, *31*, 1942–1949.

7. Kaya, S.; Uner, D. *Turk. J. Chem.* **2008**, *32*, 645-652.

8. Roldán, R. Beale, A. M.; Sánchez-Sánchez, M.; Romero-Salguero, F. J.; Jiménez-Sanchidrián, C.; Gómez, J. P.; Sankar, G. *J. Catal.* **2008**, *254*, 12–26.

9. Micheaud, C.; Marecot, P.; Guerin, M.; Barbier J. *Appl. Catal. A-Gen.* **1998**, *171*, 229–239.

10. Wu, X.; Gerstein, B. C.; King, T. S. *J. Catal.* **1992,** *135*, 68–80.

11. Uner, D. O.; Pruski, M.; King, T. S. *J. Catal.* **1995,** *156,* 60–64.

12. Uner, D.; Tapan, N. A.; Ozen, I.; Uner, M. *App. Cat. A.: General*, **2003,** *251,* 225–234.

13. Donnelly, R.G.; King, T.S. *Surf. Sci.* **1978**, *74,* 89–108.

14. King, T.S.; Donnelly, R.G. *Surf. Sci.* **1984**, *141*, 417–454.

15. King, T.S.; Strohl, J. K. *J. Catal.* **1989**, *116*, 540–555.

16. King, T.S. in *Surface Segregation and Related Phenomena*, Dowben, P. A.; Miller, A. eds.; CRC Press, Boca Raton, FL, 1990.

17. King, T.S.; Strohl, J. K. *J. Catal.* **1989**, *118*, 53–67.

18. Darby, J. B.; Myles, K. M. *Metal. Trans.* **1972**, *3*, 653–653.

19. Campbell, C. T.; Starr, D. E. *J. Am. Chem. Soc.* **2002**, *124*, 9212–9218.

20. Rousset, J. L. ; Bertolini, J. C. ; Miegge, P. *Phys. Rev. B* **1996**, *53*, 4947–4957.

21. Lide, D. R. *Handbook of Chemistry and Physics*, CRC Press, New York, 2003.

22. Løvvik, O.M.; Olsen, R.A. *J. Alloy Compd.* **2002**, *330*, 332–337.

23. Metropolis, N.; Rosenbluth, A. W.; Rosenbluth. M. N.; Teller, A. H.; Teller, E. *J. Chem. Phys.* **1953**, *21*, 1087–1092.

24. van den Oetelaar, L. C. A.; Nooij, O. W.; Oerlemans, S.; Denier van der Gon, A. W.; Brongersma, H. H.; Lefferts, L.; Roosenbrand, A. G.; van Veen, J. A. R. *J. Phys. Chem. B* **1998**, *102*, 3445–3455.

25. Hansen, P. L.; Molenbroek, A. M.; Ruban, A. V. *J. Phys. Chem. B* **1997**, *101*, 1861-1868.

26. Cheng, D.; Huang, S.; Wang, W. *Chemical Physics* **2006**, *330*, 423–430.

27. Zafiris, G.S.; Gorte, R.J. *J. Catal.* **1993**, *140*, 418–423.

28. Gracia, F.J.; Bollmann, L.; Wolf, E.E.; Miller, J.T.; Kropf, A.J. *J. Catal.* **2003**, *220,* 382–391.

29. Atalik, B.; Uner, D. *J. Catal.* **2006**, *241*, 268–275.

30. Norskov, J.K. Bligaard, T. Logadottir, A. Bahn, S. Hansen, L.B. Bollinger, M. Bengaard, H. Hammer, B. Slijivan-canin, Z. Mavrikakis, M. Xu, Y. Dahl, S. Jakobsen, C. J. H. *J. Catal.* **2002**, *209*, 275–278.

31. Uner, D.; Uner, M. *Thermochim. Acta* **2005**, *434*, 107–112.

32. Lewis, H.D.; Burnett, D.J.; Gabelnick, A.M.; Fischer, D.A.; Gland, J.L. *J.Phys.Chem. B.* **2005**, *109*, 21847–21857.